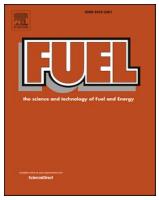
Fuel 358 (2024) 130202



Contents lists available at ScienceDirect

Fuel

journal homepage: www.elsevier.com/locate/fuel



Full Length Article



Experimental study on the flow field geometry of the PEM fuel cell bipolar plates: The effects of various shaped blocks embedded in serpentine pattern on cell performance

Selahattin Çelik [a,*], Mikail Yagiz [b,c], Fuat Yildirim [b,c], Alparslan Topcu [d]

[a] Ankara Yıldırım Beyazıt University, Department of Mechanical Engineering, 06010 Ankara, Turkey
[b] Nigde Omer Halisdemir University, Department of Mechanical Engineering, 51245 Nigde, Turkey
[c] Nigde Omer Halisdemir University, Prof. Dr. T. Nejat Veziroglu Clean Energy Research Center, 51245 Nigde, Turkey
[d] Alanya Alaaddin Keykubat University, Rafet Kayış Faculty of Engineering, Department of Mechanical Engineering, Antalya 07425, Turkey

ARTICLE INFO

Keywords:
PEMFC
Flow field
Obstacle
Performance
Impedance
Pressure drop

ABSTRACT

The flow field pattern is crucial in many aspects such as cost-efficiency (in terms of excessive fuel consumption), water management on the cathode side, and achieving a high cell performance. The studies on the reconnaissance of much more effective flow field design have been continuing for years. As a matter of fact, it may be succeeded with some manipulations on the flow area. The current research proposes to investigate the effects of blocks in various shapes and positions on the net power output by changing the shape of the channels in the flow field (FF). For this reason, semicircular and triangular blocks were machined on the serpentine channels and their short-term performances were compared with the conventional serpentine pattern. In addition to the related new FF designs, performance evaluation was made by using nickel foam placed to fill the inner part of the serpentine FF. First, ultimate operating conditions were optimized with the traditional serpentine FF. Then, the performance outputs of the proposed FF designs were compared under the same conditions assigned in the previous section. The single-cell performance tests yielded that the highest power density was ensured with nickel foam (NF)-serpentine FF with 0.267 W/cm^2. This increment corresponds to a 38 % enhancement in the power output when compared to the classical serpentine-type FF. Triangular (T) and semicircular (S) obstacles increased the performance significantly. Each manipulation on the traditional serpentine FF affected the power output positively, essentially. The pattern structures of the diagonal semicircle (DS) and diagonal triangular (DT) FFs reduced both water evacuation ability and performance increase rate. NF-serpentine FF contact highly decreased the ohmic resistance level of the cell when compared to the other designs according to the impedance (EIS) measurements. In addition, a correlation was observed between the performance and pressure drop test results. The highest-pressure drop was recorded with NF-serpentine FF (4.225 kPa) whereas the lowest is conventional serpentine FF (0.55 kPa). Traditional serpentine pattern is famous for with high-pressure drop structure. Consecutively, the pressure drop tests proved that the manipulations increased the pressure level of the system directly.

1. Introduction

Proton electrolyte membrane fuel cells (PEMFCs) are economical and reliable fuel cells due to their ability to operate in low-temperature conditions. PEMFCs consist of multiple pieces such as proton electrolyte membrane (PEM), catalyst layer (CL), gas diffusion layer (GDL), bipolar plates (BPs), and current collectors (CCs). Each of these pieces remarkably influences the performance and efficiency of PEMFC. Therefore, to increase the efficiency of PEMFC, parameters such as homogeneous distribution of gases, flow of gases, air and fuel ratio, and removal of water formed during the chemical reaction must be optimized. These parameters can be improved with a bipolar plate design with an efficient flow field pattern [1]. In general, the purpose of flow field designs is to ensure that the reactants (hydrogen and oxygen) are transported to the catalyst layer through channels and to prevent the accumulation of reaction products in the CL structure. Thus, the influence of different gas circulation patterns on the PEMFC peak power density is an important issue. Although there are characteristic flow field

* Corresponding author.
E-mail address: selahattincelik@aybu.edu.tr (S. Çelik).

https://doi.org/10.1016/j.fuel.2023.130202
Received 25 August 2023; Received in revised form 14 October 2023; Accepted 26 October 2023
Available online 31 October 2023
0016-2361/© 2023 Elsevier Ltd. All rights reserved.

designs in the literature in general, the commonly used PEMFC flow channel types are serpentine, interdigitated, and parallel channels. The serpentine gas flow field designs are the most preferred design in trading PEMFC stacks due to their low material cost and high fertility in production [2]. In addition, different gas flow field designs such as tubular, spiral, pin, cascade, bio-inspired, and 3D (three-dimensional) have also been tested in some studies and the results have been reported [3–6].

Recently, many researchers have performed studies to increase the performance of PEMFC by designing characteristic flow fields. Chadha et al. [1] compared PEMFC performance with two new BP designs with multi-serpentine and hybrid flow patterns under the same pressure ratings. Atyabi et al. [2] investigated the multiphase model of a PEMFC with a honeycomb flow area on the cathode side. It is reported that the pressure decreases along the cathode flow area, and accordingly, the pressure and temperature distributions are regular at the interface of CL and GDL components. Chen et al. [3] constructed a multi-phase PEMFC model with a new wave flow channel design. The geometric structure of the flow area was optimized and the current density (A/cm^2) in the new flow field was found to be 23.8 % higher than the traditional flow field under 0.4 V operating condition. The influence of undulating flow field design on PEMFC performance was experimentally investigated by Anyanwu et al. considering serpentine, straight parallel, and interdigitated FFs [5]. It is stated that optimizing parameters such as relative humidity level, activation resistance, and charge transfer rate could increase cell performance for all FF designs. Zhou et al. conducted a series of studies [6–8]. They performed simulated research on sinusoidal wave-flow channel design [6]. This study examined the effect of sinusoidal wave function amplitudes and periods on PEMFC performance. As a consequence, they reported that the reverse wave flow channel outperformed the straight flow channel in terms of mass transfer capacity. In another study, the effect of opposing sinusoidal wave FF (OSWFF) and parallel FF on water and gas flow for the cathode flow field of PEMFC was explored [7]. The inlet sections of the flow fields were supported with trapezoidal obstructs to increase the homogeneity of oxygen. OSWFF, gas transfer, and water removal performance showed better results (9.30 % at 2.2 A cm^{-2}). In another study by Zhou et al. [8], a new FF was created to understand the effect of water and gas fluids in PEMFCs. The novel FF exhibited a positive output on water removal. It also improved the homogeneity and velocity uniformity of oxygen by 7 % and 28 %, respectively. Weng et al. [9] proposed FFs to evaluate and compare their performances with classical serpentine FF. They considered both sides of the cell including the anode and cathode conditions, and the 3D fine mesh pattern was found better than the wire mesh and metal foam structures. Besides, it was reported that the fine mesh and metal foam have the potential to dissipate huge water droplets. In another study, a novel FF with metal foam was proposed for the cathode compartment by Wan et al. [10]. The effect of the metal foam height (1 to 5 mm) on the thermal properties of an air-cooled stack was investigated. As the metal foam height increased, the average temperature of the stack decreased by 8.4 °C, and the efficiency level of the system rose by 14.7 %.

Qin et al. [11] proposed large-scale FF designs with low pumping losses to optimize the cathode BP in PEMFC. They created three novel patterns by the combinations of parallel, baffled, serpentine, and narrow patterns and tested them. The baffled FF improved the performance by 23 % with low pumping loss. Valino et al. [12] performed a numerical study to examine the distribution of fuel (hydrogen) and air (oxygen) gases at the inlet locations of a PEMFC bipolar plate. Chowdhury et al. [13] achieved better cell performance with the newly designed serpentine FF. A new serpentine channel design has been obtained by changing the channel depths of the pattern. Cell performances were investigated regarding the traditional serpentine flow channel and they provided a 19–27 % power increase. Li et al. [14] aimed to increase the mass transfer of PEMFC by designing a key-shaped 3D (three-dimensional) flow channel. The power density has been increased by about 30 % from the better block size. Dong et al. [15] examined the influence of five characteristic obstruct patterns on mass transfer and flow to increase the performance of a PEMFC. It has been suggested that the blocks placed in the flow area increase the mass transfer due to the nozzle type effect. Hsieh et al. [16] investigated the effect of pressure lower in four different gas flow channels, namely serpentine, parallel, interdigitated, and mesh type, on the flow distribution depending on temperature and air flow rate for PEMFCs. Kerkoub et al. [17] researched the influence of channel width and the ratio between ribs on PEMFC performance with the help of the 3D-CFD (three-dimensional-computational fluid dynamics) model. He et al. [18] designed the S-series flow channel and experimentally investigated the cell performance effect of this series. They achieved a 15 % increase in power output. In another study, Dong et al. [19] improved the performance of a PEMFC by adding discontinuous S-shaped and crescent ribs to flowing channels. Wang et al. [20] examined three types of reactant flow field design, both numerically and experimentally, on the performance of PEMFC.

The cross-flow stem from the staggered trapezoidal baffle plate (STBP) flow area arrangement improved the homogeneous dissipation of the reactant and increased the PEMFC power level in different operating conditions by removing excess water from the porous electrode. Chen et al. [21] experimentally investigated the effect of baffle leeward length on power density and pressure loss in PEMFCs. It has been reported that pressure drops decrease when longer baffle lengths are added to the channels. Shen et al. [22] worked on the performance of PEMFC by placing four characteristic barriers in the conventional serpentine gas flow channel. It has been noted that the synergy angle between the gas velocity and the concentration at the cathode decreased with the addition of blockages, the coefficient of mass transfer improved, and thus the power level of the PEMFC was increased. Wilberforce et al. [23] conducted extensive research on the effect of BP channel patterns on the power output of PEMFCs. They discussed the utility of an FC system using different and characteristic types of BPs. The benefits and defects depending on BP geometry design were also reported.

Wang et al. [24] applied various conventional FFs which are parallel, pin, and metal foam to the cathode side and investigated their performance specifications depending on the operating conditions, experimentally. Open cathode PEMFC stack was analyzed and polarization curves (current–voltage) and electrochemical impedance spectroscopies (EIS) of the case studies were measured and compared. It has been specified that the metal foam-based FF showed the best output performances compared to the other flow fields. Sadeghifar et al. [25] claimed that a channel design called the trap flow channel, would increase the power density of PEMFCs. The effect of this trap-shaped flow channel was studied through a non-isothermal 3D model via ANSYS Fluent. He et al. [26] designed a novel FF that consists of randomly placed 3D trapezoid geometries. The designed 3D FFs supported stack power output, particularly at elevated current levels. It has been reported the performance of 3D FFs developed by 15 % compared to the conventional parallel FF. Palaniswamy et al. [27] machined various flow patterns which are classical serpentine, pin type, and uniform on the cathode BP. In addition, a 2 mm cubic porous carbon structure was used in FFs except for the serpentine type. It is reported that the addition of porous carbon along the flow channel surface of the pin-type FF has better water transport ability.

The issue was investigated in many aspects both experimentally and numerically as presented in the literature survey above. However, this process is an endless endeavor and will last as long as fuel cell life in our environment. In this work, as a different from the available studies, various-shaped blockages were placed into the serpentine channel and their effects on the cell performance were investigated experimentally. The serpentine flow fields with semicircular and triangular blocks were prepared and their single-cell performance test results were compared with a conventional serpentine one under the same operating conditions. Besides, a metal foam was filled to the bottom side of the

traditional serpentine channel and evaluated in terms of cell performance. The optimum operating parameters were determined with a conventional single-serpentine flow field, and then, all designed flow patterns were tested under the specified conditions with single-serpentine. Therefore, a correct performance evaluation was ensured between the flow field patterns. In addition, pressure drop tests were performed as well as short stack tests. Thus, cell performance and pressure drop relation were discussed.

2. Experimental

2.1. Flow field design details

Short-stack tests were performed using a commercial membrane electrode assembly (MEA) in the studies [28]. MEA used in cells has an active area of 25 cm^2. The structure consists of a combination of gas diffusion, catalyst, and membrane. Therefore, the dimensions of the BPs were assigned depending on the active area of the MEA. Flow fields based on traditional serpentine geometry with blocking were designed using 3D technical drawing software. Then, the designed variations of the single-serpentine FF were machined using a metal laser cutting device (Durma Brand Laser Cutting Device, USA). Based on the traditional serpentine flow field, four different flow fields with two different flow barriers were designed. Bipolar plates with the proposed designs were applied to both anode and cathode compartments. Therefore, bipolar plates were manufactured as a couple for both sides. In addition, a porous metal nickel foam is placed in the serpentine flow channel. The metal foam used in the flow channel is made of nickel material (Zopin Group Co., Ltd, Xiamen, China). The porosity of the nickel metal foam material is in the range of 95–98 %, the thickness is 1 mm, and the purity is about 99.99 %. The desired flow area size was cut in the dimensions to be placed in the serpentine channel. Fig. 1 shows Nickel metal foam sample for experiments (Fig. 1-a) and the pore structure (Fig. 1-b) obtained with the aid of a microscope (Leica EZ4 W, Leica Microsystems, Germany).

All the BPs are made of copper and presented in Fig. 2. In the figure, conventional single-serpentine, serpentine filled with nickel foam, semicircular blocked, triangular blocked, diagonal semicircle blocked, and diagonal triangle blocked FFs were illustrated, respectively. Besides, flow field and blockage dimension details were provided in the same figure. The specifications of the investigated FFs and the characteristics of the short stack used in the tests are given in Table 1. Plexiglass was preferred as an end plate material and prepared with 100 * 100 mm^2 in dimensions and 10 mm in thickness. The current collectors are used for the collection of the current generated in the cell, in general. However, these components were eliminated in the current study, and the current was drawn from the cable shoes placed on the corner of each BPs as seen in Fig. 2. Different flow field designs used in this experiment were brought to the cell right and fixed with eight bolts. A torque of 5 Nm was applied to each bolt with the help of a torque meter during the assembly process to sustain better connectivity and maximum sealing between the flow fields and the MEA.

All the dimensions of the BP and BP active area were kept constant and equal. Therefore, the channel structure was designed depending on the active area conditions. For each FF 12 turns were created in the area and the entire size of the channel of the channel was calculated as 674 mm. The channel depth and width were assigned as 1 and 2 mm, respectively. The blockage number on the channels and the other related specifications are illustrated in Table 1.

2.2. Cell performance tests

2.2.1. Test equipment and conditions

Initially, the activation procedure was applied to obtain a stable voltage from the commercial membrane [29]. The fuel cell test station model (Arbin Instruments, FCTS-800, Texas, USA) where the tests were carried out was used (Fig. 3-a). At first, the operating conditions were fixed with single-serpentine FF, then the other designed FFs were tested under the same conditions. In order to create the desired operating temperature (Fig. 3-d), an air-conditioning cabinet (ESPEC Corp, SH-221, Japan) where both temperature and humidity control can be made together was used, and humidification was provided by an external loop. The water that existed in the cylinder was warm-up until 50 °C thanks to a hot plate mechanism (Fig. 3-d). The H_2 passed through the warmed water and therefore the humidified H_2 was ensured to the cell.

2.2.2. Specifying the optimum operating temperature

Before starting the comparison tests for the novel FFs, operating conditions were specified with the classical serpentine FF. Then, the short stack was operated at 30, 40, and 50 °C temperatures with 3:1 air/fuel stoichiometry. The PEM fuel cell is operated between 60 and 80 °C, normally. However, the humidity balance of the MEA may not be supplied successfully at higher operating temperatures. In case of any instant change experienced in the humidity, it leads to performance degradation in the cell easily. Hence, the FF pattern effect on the cell performance may not be distinguished since the humidification problem dominated and affected the power output of the cell, directly. In this context, the test temperature of the case studies is relatively lower when compared to the normal operating conditions of the PEM fuel cells. This case is going to reveal the effect of proposed FFs on the cell performance output, clearly. In addition, all proposed FFs were tested as well as the classical serpentine type at the same operating temperatures.

2.2.3. Specifying the optimum gas ratio

With the assigned optimum cell operating temperature, then, the

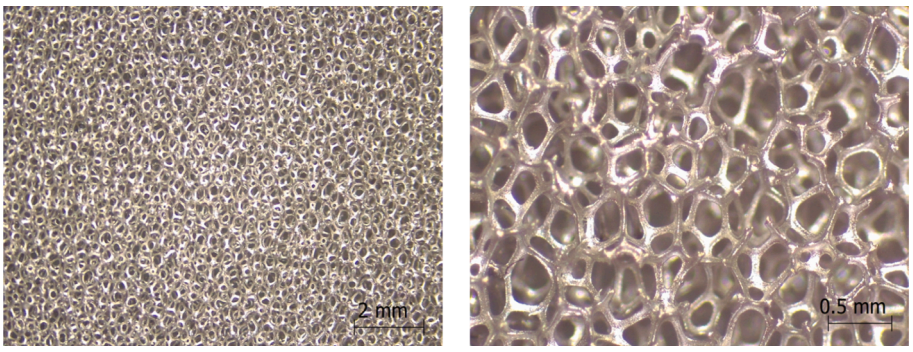


Fig. 1. (a) Nickel metal foam sample used in the serpentine ff, (b) closer view pore structure of nickel metal foam.

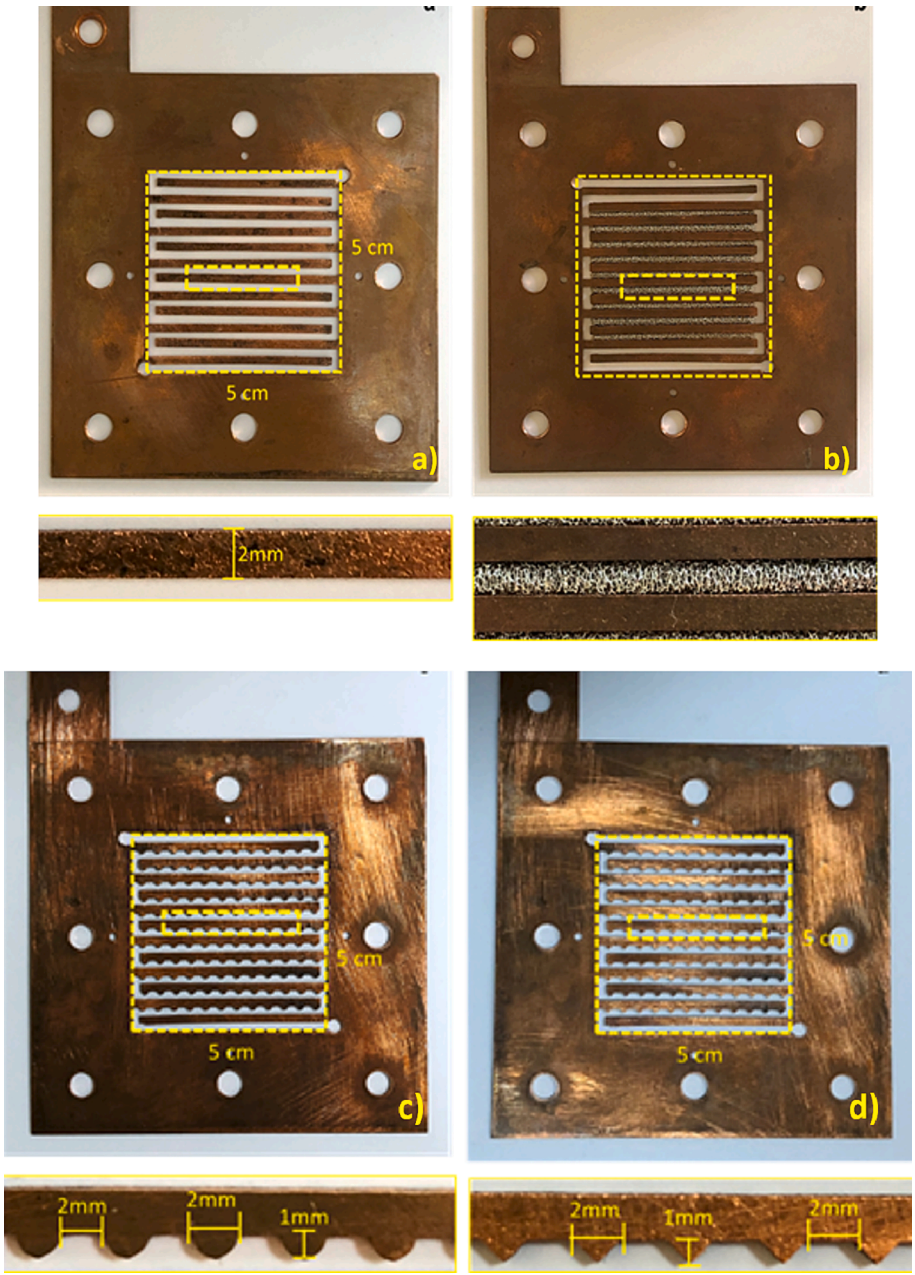


Fig. 2. Flow field patterns; (a) Serpentine (SR), (b) NF-serpentine (NF), (c) Semicircular (S), (d) Triangular (T), (e) Diagonal Semicircle (DS), (f) Diagonal Triangle (DT).

short stack was tested at various air/fuel stoichiometries. First, the stoichiometry was determined considering the operating parameters presented in Table 2. Then, H_2 and air gas ratios were evaluated to specify the optimum gas flow rates. 0.3/0.9, 0.4/1.2, 0.5/1.5, 0.6/1.8 0.7/2.1 lt/min H_2 and air gas ratios were assigned. Polarization curves were obtained after each test and therefore the maximum power output of the stack is determined by changing the reactant and oxidant gas ratios.

2.2.4. EIS measurements

The electrochemical impedance spectroscopy (EIS) measurement results support the performance results, and the losses in the cell were investigated by measuring the ohmic, charge transfer, and mass transfer resistances for oxygen reduction. Electrochemical impedance spectroscopy (EIS, Parstat 2273, Oak Ridge, USA, Fig. 3-b) was performed with supporting impedance outputs of the cells were also obtained at the same temperature and in reactant ratio of H_2/air (1:3). Under the open circuit potential, each flow field was measured in the frequency range of 0.1 Hz–250 kHz and compared.

2.2.5. Pressure drop tests

The pressure variation in the flow region is an important parameter in the evaluation of the reactant flow field geometry. An available optimized flow channel structure ensures proper distribution and removal of reactants and products. In the serpentine design, in both the anode and cathode active area, air and H_2 gases are forced to flow in a single path, which can consist of a long flow channel across the surface area with a single inlet and outlet. This creates a pressure drop across the flow channel due to both flow velocity and friction in the channel walls. The obstacles placed in the serpentine channel and their locations may

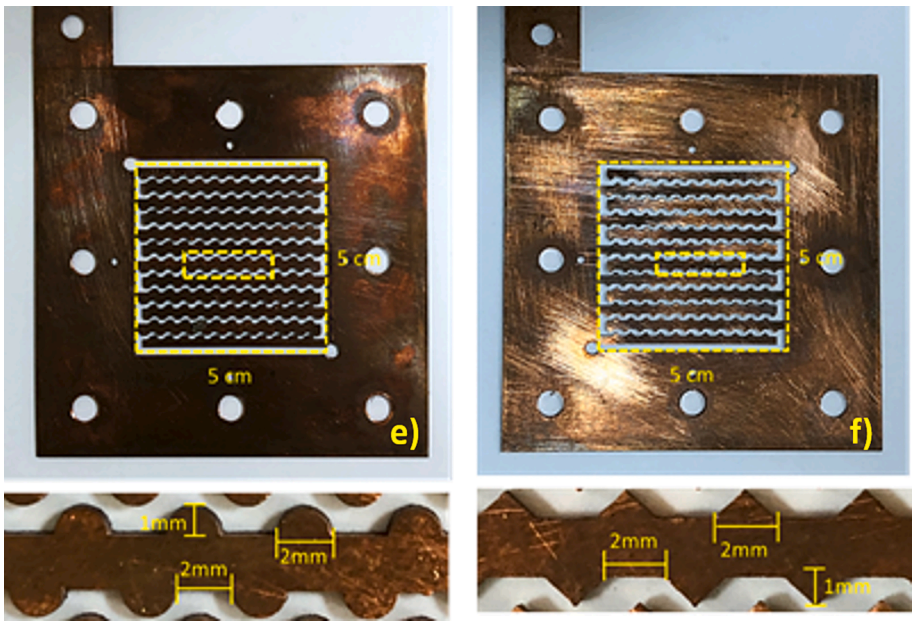


Fig. 2. (*continued*).

Table 1
Geometrical parameters of the designed flow fields and short stack specifications.

Flow field pattern	SR	S	T	DS	DT
BP Material	Copper metal	Copper metal	Copper metal	Copper metal	Copper metal
BP Dimensions (mm)	100 * 100 * 1	100 * 100 * 1	100 * 100 * 1	100 * 100 * 1	100 * 100 * 1
Num. of Turn in Channel	12	12	12	12	12
Total Channel Length (mm)	674	674	674	674	674
Active Area (cm^2)	25	25	25	25	25
Channel Depth (mm)	1	1	1	1	1
Channel Width (mm)	2	2	2	2	2
Rib/Land Width (mm)	2	2	2	2	2
Block Width (mm)	–	2	2	2	2
Block Length (mm)	–	1	1	1	1
Block Number	–	132	132	253	253
End Plate Material	Plexiglass	Plexiglass	Plexiglass	Plexiglass	Plexiglass
End Plate Dimensions (mm)	100 * 100 * 10	100 * 100 * 10	100 * 100 * 10	100 * 100 * 10	100 * 100 * 10

SR: Serpentine, S: Semicircle, T: Triangle, DS: Diagonal semicircle, DT: Diagonal triangle

affect the transmission of air and H_2, increase the homogeneity of the substance distribution in the area, and facilitate the removal of the liquid water formed during the reaction in the cathode region. As a result of all these situations, it may increase the performance of the cell. Alicat (Alicat Scientific, Tucson USA) brand gas flowmeter, with a response time of less than 100 ms, precise control of flow and pressure changes is achieved. In this context, pressure drops of nickel foam (NF) placed in the serpentine FF, and semicircle (S), triangle (T), diagonal semicircle (DS), diagonal triangle (DT) FFs, and traditional serpentine FF were determined.

3. Results and discussions

3.1. Effect of temperature on performance variation

The increased operating temperature through the climatic chamber helps to improve the cell performance due to the electrochemical reaction in the PEMFC, in general. PEMFC performance varies depending on the temperature at which the cell is operated. With the gradual increase in temperature, the conduction of gases, reaction kinetic energy, and membrane conductive potential values increase greatly. When the studies are examined, the operating temperature of the cell is an important parameter in increasing the performance [30,31]. To observe the effect of operating temperature on the performance of the fuel cell, three different relatively low operating temperatures were tested, and the operating relative humidity of the reactant H_2 gas was considered as a constant 50 °C. The cell performance increased with the increase of operating temperature as seen in Fig. 4-a. The maximum power density value of 0.194 W/cm^2 was reached at the constant 50 °C operating and humidification temperature of the cell. 0.179 and 0.145 W/cm^2 power densities were recorded at 40 and 30 °C test temperatures, respectively.

On the other hand, the operating temperature effect was evaluated considering all proposed FFs. Peak power densities of the FFs at specified temperatures are illustrated in Fig. 4-b. The highest performance was achieved with NF-serpentine type as 0.267 W/ cm^2 at 50 °C. 0.249 and 0.208 W/cm^2 power densities were recorded for the NF-serpentine at 40 and 30 °C test temperatures, respectively. The reached power density levels of the NF-serpentine FF are noticeably higher than the conventional serpentine type at the specified test temperatures. The second highest performance was recorded with semicircle FF as 0.225 W/ cm^2 at 50 °C. Actually, any manipulation to the flow pattern increased the cell performance. The power density values of the classical serpentine (0.194 W/ cm^2 at 50 °C) are lower than the lowest performance of the proposed FF which is the diagonal triangle (0.199 W/ cm^2 at 50 °C). Herein, the test results of the serpentine-type FF is not shown in Fig. 4-b since it is presented in Fig. 4-a already.

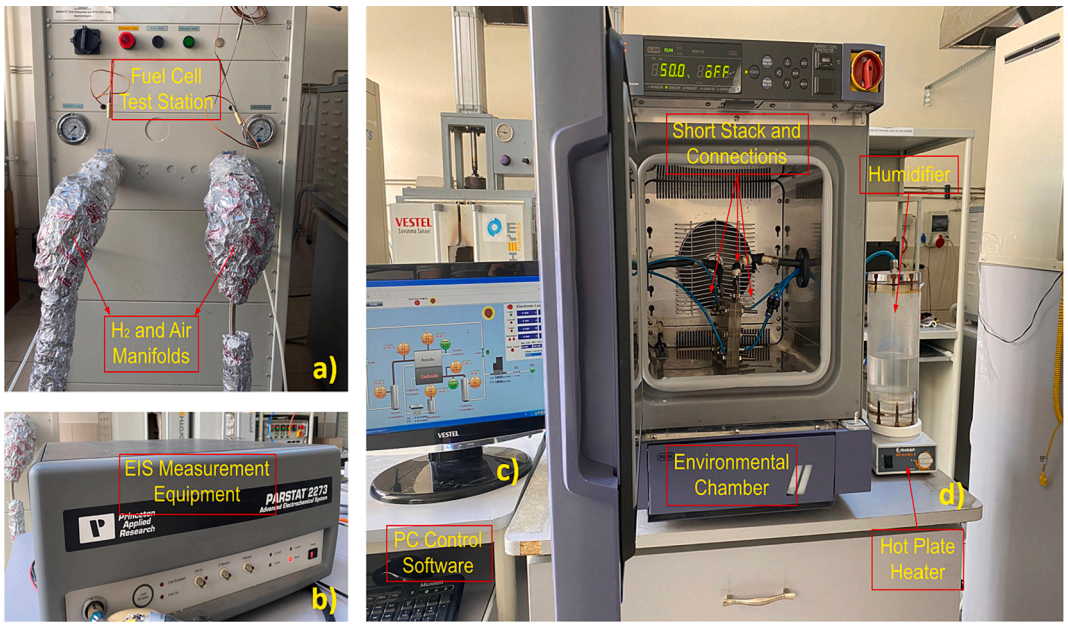


Fig. 3. Schematic of the experimental setup.

Table 2
Air/fuel stoichiometry test parameters.

Test #	H_2 Flow Rate (lt/min)	Air Flow Rate (lt/min)	Cell and H_2 Humidification Temperature (°C)
Case 1	0.6	0.6	50
Case 2	0.6	1.2	50
Case 3	0.6	1.8	50
Case 4	1.2	0.6	50
Case 5	1.8	0.6	50
Case 6	1.8	1.2	50
Case 7	0.6	2.4	50

Since the water content in the membrane generally decreases at operating temperatures of 60 °C and above, the tests were conducted in non-humid conditions. That is, the membrane is adequately hydrated in high relative humidity conditions, while it is not sufficiently hydrated in low relative humidity levels. This causes the drying of the MEA and the decrease in ion conductivity. Therefore, lower operating temperatures were preferred to ensure that there was enough water in the membrane [32–35]. When the operating temperature exceeds the humidification temperature, the amount of water in the active area will increase during the reaction. The increased amount of water will both clog the diffusion layer pores and cause overflow [36]. Thus, it causes a decrease in performance, again. Therefore, the operating temperature was not increased further.

3.2. Determining the optimum gas ratio

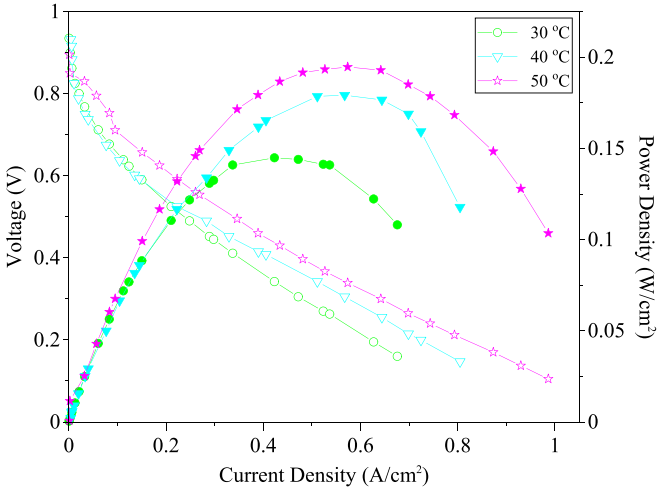
After completing the optimum operating temperature section, air/fuel stoichiometry was determined considering the test parameters presented in Table 2. Short-term test results of the case studies are demonstrated in Table 3. The highest power density was achieved by 1:3 stoichiometry (Case 3) as seen in Table 3. Therefore, rich air and sufficient H_2 gases are required for the maximum power. Increasing the total amount of air in the cathode reaction zone provides more oxygen demand to the catalyst open area during the chemical reaction. It also helped to remove excess air and water from the reaction zone. When the air velocities were increased further, it quickly left the cell from the reaction sites without having enough time to participate in the reaction. Thus, a slight decrease in performance was observed in case 7 compared to case 3. Similarly, as in case 4, when the amount of H_2 supplied from case 1 to the anode flow region is increased, this situation where the power density increases is probably due to the lack of H_2 for the reaction. As a result of further increasing the H_2 velocity in case 5, the scavenging of the reaction gas on the anode active surface causes the relative humidity to decrease. Thus, the proton exchange has affected the drying of the membrane. As a result, it caused a decrease in performance due to mass transfer. For the cathode, cases 1, 2, and 3 respectively, the power density increased as the amount of air increased. However, although the increase in the air ratio in case 7 removed the amount of water produced, the power density decreased somewhat because it caused the membrane to dry out. Depending on these performance results, the performance of the reactant ratio (H_2/air: 1/3) at different flow rates was investigated by taking the serpentine flow remainder as a reference.

Then, the calculation of the optimum H_2/air flow rate is essential to inhibit both excessive fuel consumption and degradation of performance. The polarization curves depending on the various H_2 and air flow rates were created and presented in Fig. 5. It is understood that the best performance was obtained with the 0.6/1.8 lt/min ratio. In this case, the water level formed at the cathode as a result of electrochemical reactions in the serpentine flow channel changes depending on the H_2 and air ratio and the hydrogen and air flow rates sent at the same reactant ratio. Due to the excessive increase in the amount of liquid water formed in the cathode area, it caused low ionic conductivity. For this reason, the optimum performance effect in the flow channels was investigated by using 0.6/1.8 lt/min gas ratio and H_2/air ratio.

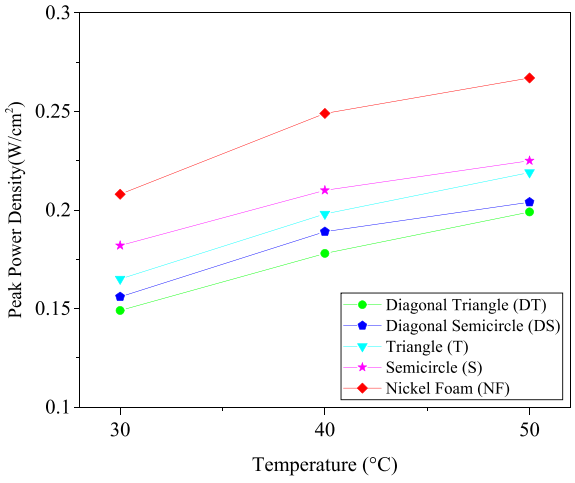
3.3. The effect of serpentine flow field geometric structure on performance

The current and power densities of the PEMFCs with the designed various shaped FFs were calculated and plotted. In Fig. 6, the polarization curves of the designed FFs are illustrated.

It is seen clearly that any disturbance on the serpentine channel



a)



b)

Fig. 4. (a) Polarization curves for different temperatures at single serpentine ff, (b) peak power densities of designed ffs at different temperatures.

Table 3
Air/fuel stoichiometry test results.

Test #	H_2 Flow Rate (lt/min)	Air Flow Rate (lt/min)	Maximum Power Density (W/cm^2)	Cell and H_2 Humidification Temperature (°C)
Case 1	0.6	0.6	0.151	50
Case 2	0.6	1.2	0.176	50
Case 3	0.6	1.8	0.194	50
Case 4	1.2	0.6	0.157	50
Case 5	1.8	0.6	0.146	50
Case 6	1.8	1.2	0.164	50
Case 7	0.6	2.4	0.187	50

resulted in positive power output. Triangle and semicircle installation to the serpentine FF highly improved the performance relative to the diagonal triangle and diagonal semicircle blockages. It puts the importance of blockage shape on the cell performance. The presence of

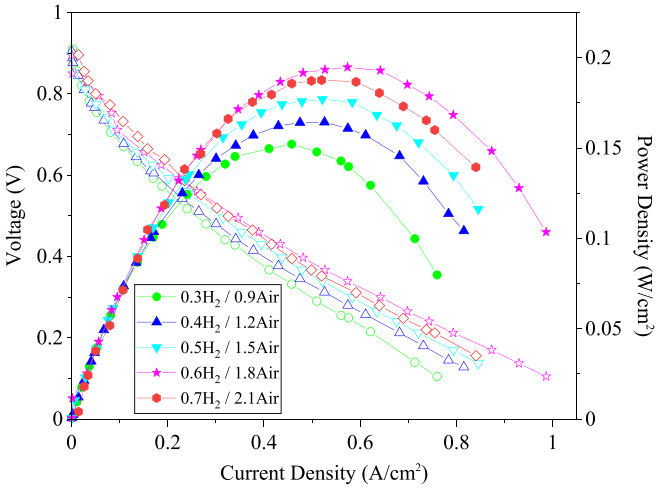


Fig. 5. Polarization curves at different H_2/Air ratios with single-serpentine FF.

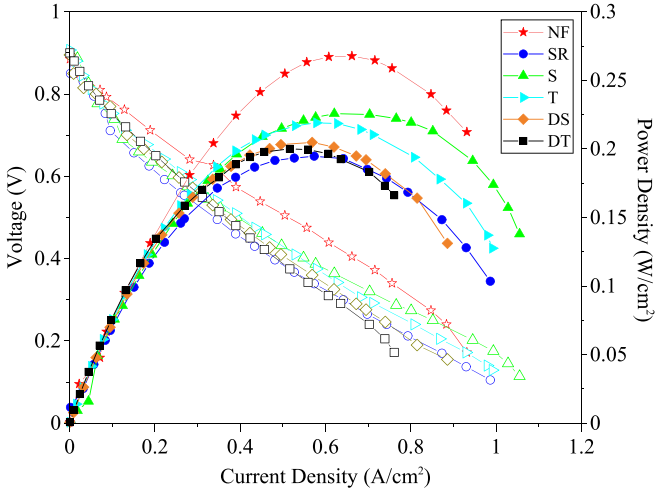


Fig. 6. Polarization curves of designed FFs.

obstacles in the channel basically facilitates the transition of reaction gases to the gas diffusion layer (GDL) and increases the concentration of oxygen in the catalyst layer. It also helps retain liquid water within the channels at high flow rates, which increases membrane hydration and improves protonic conductivity. As a result, the reaction occurs faster, making the current density higher [37–39]. Current density is affected by mass transfer in the PEMFC system and herein is affected by mass transfer through the barrier state in flow channels. The reactant in the active sites of the porous media (GDL) was triggered, the contact point number was increased and the electrochemical reaction was forced to improve with the attaching of both barrier shapes (triangle and semicircle) to the flow channels.

Also, the mass transfer behavior changes when changing the position of the baffle shapes (semicircle/diagonal semicircle and triangle/diagonal triangle). When the obstacle is brought to their cross position, the fluid flow properties around the chambers also change, and accordingly, the transport state of the reactant gases and the water produced in the cathode region along the flow area and the states formed along the channel also change. Consequently, this affects the electrochemical reaction rate in the catalyst layers of the MEA. The semicircle (S) FF has a slightly higher performance when compared to the semicircular triangular (T) since the flow is smoother at the extreme points. As the radius of the water droplet formed in the conventional serpentine flow channel increases, it takes longer for the droplet to flow out of the straight

channel. Depending on the GDL surface, it clogs it to a certain extent and moves away in the monoblock channel. However, while the water formed as a result of the reaction moves in the semicircle (S) and triangular (T) flow areas, the obstacles slow down the flow rate relatively. Compared to straight channel SR, monoblock channels will cause the flow rate to increase in the gaps where there are obstacles with the GDL surface due to the narrowing of the flow channel around the block. While water droplets pass through the hydrophilic surface and the parts where there are obstacles, the acceleration force when passing through the GDL surface breaks the droplets into small sizes in these parts. As droplet sizes decrease, the adhesion force applied to the surface will decrease and its resistance to high air flow will decrease. Single-sided S and T barriers provide both an acceleration effect and droplet fragmentation, removing water droplets on the GDL surface, thereby opening the pores and ensuring the continuity of the electrochemical reaction [40,41]. A 16 % increase with semicircle FF and a 13 % increase with triangular FF was achieved in the net power output when compared to the traditional serpentine FF performance under the same operating conditions.

DS and DT FFs showed close performances due to the mutual cross-location changes of blocks. Nevertheless, they led to higher performance than the conventional serpentine FF. The areas around the obstacles where the fluid flows are narrower and the flow velocities increase further and the inertia effect on the water flow is strengthened in the DS and DT types in case of an increase in obstruction in the flow area. Compared with straight SR channel and unilateral semicircle and triangular obstacle channel, cross semicircle and cross triangular obstacle FF channel has more advantages in terms of water removal. Because the presence of more obstacles on the GDL surface of the droplets can continuously increase the flow rate and cause the water droplets to separate earlier before growing. Therefore, the water is swept from this region effectively and easily. As a result, the produced water can be removed successfully from the porous media but the concentration in cell polarization decreased. It is obviously stated that the DS and DT designs help to water removal in the channels but their impact on the power output of the cell is weak according to the semicircle and triangle-shaped configurations. It is seen that the current level of the DS and DT designs decreases especially in higher current regions under the 0.3 V. The cell needs fresh H_2, especially at higher current concentrations which can be explained by reactant starvation. The structure of the diagonal designs is not appropriate to satisfy this expectation. The mentioned issue is related to the pressure drop behavior of the patterns, and the relation is explained in that section. Thus, the diagonal flow fields are incapable especially at higher current drawn levels, and they exhibited lower performance output than the serpentine type.

It is clearly seen in Fig. 6 that the highest performance was ensured with the nickel foam-serpentine FF coupling. 0.267 W/cm^2 maximum power was achieved and a 38 % increase was supplied with the NF-serpentine FF when compared to the conventional serpentine FF. It puts the effective output of the collaboration of nickel foam and serpentine FF relation.

3.4. EIS measurements

To further investigate the serpentine flow field effect, the shape, and location of the blockages placed in the serpentine channel were also compared with the metal nickel foam electrochemical impedance data placed inside the straight serpentine channels. The configuration in Fig. 7 shows differences in the EIS graphics as a result of the design changes. In general, the ohmic resistance is low in PEM MEA. As presented in Fig. 7, all the measured resistance values can be accepted as low levels. It is found as lowest for nickel foam-serpentine FF. The main reason for this is to prevent gas flow in the channel and to provide homogeneous distribution throughout the active area. Close measurements were recorded for the triangle-semicircle and diagonal triangle-diagonal

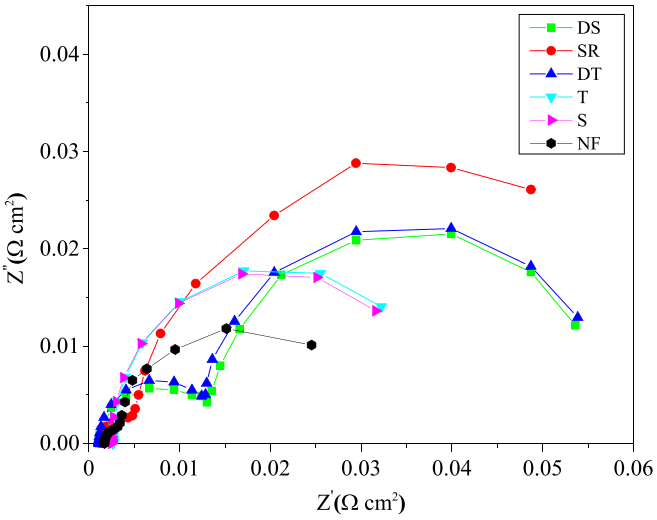


Fig. 7. EIS measurements of the designed FFs.

semicircle FFs. The situation here is that due to the increase in the number of obstacles in the flow channels given in Table 1, the accumulation of water formed as a result of electrochemical reactions in the channel, and its flow is prevented. Accordingly, the reduction of the air passage in the GDL and the slowing of the oxygen reduction reaction. The differences in resistance values originate from the passage of oxygen ions through the membrane and the contact resistance between the electrode/electrolyte and the electrode/current collector layer.

3.5. Pressure drop measurements

The serpentine flow geometric structure provides easy transmission of H_2 in the anode region and air in the cathode region. The single channel structure in the active area limits the uniform transmission of the dispersion of the reactants. This structure is characterized as an advantage in removing liquid water from the cathode. But in-channel blocking design causes a rapid collision between gas and channel surface. In addition, it has a higher pressure drop in the active area and increases the pump power requirement for transmission. All these situations cause a performance change in the fuel cell. Pressure drop is the natural result of the flow channel structure, and is reduced an amount through the circulation of fluids in the channels. The pressure drop across flow channels is mainly caused by two effects: (i) the number of obstacles in the channels, their shape, diameter, etc. properties, and (ii) surface friction. In channels where there are no obstacles, the pressure drop occurs as a result of surface friction caused by laminar flow. This pressure drop is directly proportional to the mass flow through the channels [39]. In channels with obstacles, the pressure drop depends on many parameters. However, the number of obstacles in the channel and their settlement pattern are the most effective parameters. In general, increasing the number of barriers increases the distribution of gas reactants within the channel, resulting in an increase in cell performance [42]. However, considering the number of obstacles in the flow channels in Table. 1, it was observed that the pressure increase was lower in the DS and DT channels, which have more obstacles, than in the S and T channels. The water formed as a result of the reaction of the reaction gases must be removed from the channel without clumping. The sequential arrangement of the obstacles in the S and T channels enables the flow of water from the cluster and ensures the flow rate and homogeneous distribution of the reaction gases better than DS and DT. The flow of reaction gases slows down, probably because the mutual arrangement of DS and DT allows local accumulation of water. Accordingly, the pressure drop decreases as a result of regional blockages. Pressure drops (in kPa units) of the designed FFs were presented in

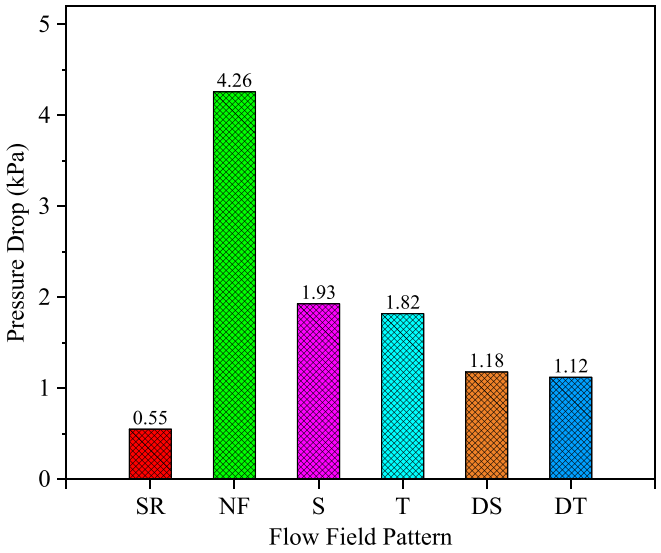


Fig. 8. Pressure drop of designed FFs.

Fig. 8. The highest pressure drop value was recorded with Nickel Foam -Serpentine FF (4.225 kPa) whereas the lowest was performed with conventional Serpentine (0.55 kPa). This is because channel blockages lead to higher flow resistance, thus accelerating electrochemical reactions. It is proven that the settlement of any obstacle on the serpentine FF or addiction of foam layer increases the pressure drop. Semicircle and triangle designs also increased the pressure drop when compared to the initial (classical) serpentine flow field shape. The reason for this is that the blockages formed by the water drop on the surface cause more flow resistance and losses. Reducing the obstruction in the channel accelerates the electrochemical reactions and causes an increase in the amount of liquid water produced by the channel [43]. High pressure is the natural result of a serpentine channel design. Because the channels have U-turns throughout the circulation and it leads to pressure losses through the flow.

A higher performance was achieved with the NF serpentine couple. Correlatively, the pressure drop value of this design is the highest. A similar trend was observed in the other designs. Also, the relationship between channel obstructions and pressure drop is shown in Fig. 8. The position and structure of the blocks and nickel foam placed in the serpentine channel clearly affected the pressure drop and power density.

3.6. Time-dependent power density variation at constant voltage

Experimental measurements to examine the effect of different flow channels on power density were carried out considering the optimum operating conditions (50 °C and H_2/air: 0.6/1.8) where the best performance was achieved. It is difficult to distinguish between the flow rate of reactants and the formation processes of products in the anode and cathode flow regions. For this reason, the same flow field designs were applied to both electrodes. Water formation occurs as a result of the electrochemical reaction of reactant gases at the electrode. The water formed at the cathode electrode is collected in the gas diffusion layer and flow channel. Management of the water formed here is an important situation that affects cell performance. Since the formation of water is an electrochemical process, ambient temperature has a significant effect. Since the temperature increase increases the reaction kinetics, the amount of water formed per unit time will increase. However, as a result of the reaction, water in gaseous form accumulates in the flow channels over time. Under the effect of the air flow in the cathode flow channel, they will coalesce towards the outlet of the channel and become small water droplets [44]. The presence of accumulated water will reduce the flow rate of the reactant. It will cause an increase in pressure within the channel. This situation varies depending on the configuration of the flow channels. It is shown in Fig. 8 that the total pressure drop in serpentine flow areas is the least compared to other flow areas. In laminar flow structures such as serpentines, the pressure drop resulting from the surface friction effect is directly proportional to the mass flow rate passing through the channels. The change in mass flow rate changes the current and power density over time depending on the current. At low voltage and high current densities, reactant consumption rates in the flow channels are high.

The plots in Fig. 9 show the H_2/air ratio of 0.6/1.8 (lt/min) at a constant 0.4 V between 0.3 V and 0.7 V [45] at 50 °C cell and humidity temperatures to ensure operation in the highest performance range. shows the variation of power densities after a constant 1200 s operation.

When the Serpentine flow field design started to work, the power density was measured as 0.191 (W/cm^2), and it was recorded as 0.186 (W/cm^2) after about 1200 s. In general, it remained stable in short-term operation. When the other designs were examined, the rate of change in power densities at the beginning and after 1200 s, respectively, was approximately 5.1 % in diagonal triangle, 5 % in diagonal semicircle, 4.4 % in triangle, 4.2 % in semicircle and 10 % in nickel foam. Herein, although the obstacles in the flow channels generally increased the performance, the blocks contributed to the formation of puddles. Nickel foam placed in such a way as to fill the channel in nickel foam, where the highest performance decrease was observed, generally contributed to the homogeneous distribution of the reactants. However, it accelerated the condensation of water droplets in the entire channel, causing blockages along the channel and then a decrease in power density.

4. Conclusions

In order to increase the performance of PEMFC, blockages in different shapes and positions have been proposed to the serpentine anode and cathode flow channel. Nickel foam (NF), semicircle (S), triangle (T), cross semicircle (DS), cross triangle (DT) obstacles placed in the serpentine flow area, taking the straight single serpentine flow channel as a reference, H_2 and air velocities, constant rates, temperature, pressure drops and long-term operating conditions were analyzed with EIS and performance measurements. In addition, flow field design is of vital importance for water management and flooding problems as a result of reaction in the active area, which is one of the most important problems during the study. In the present experimental study, the benefits of obstacle usage on the power output of the system were proved. Designed various obstacles were placed into the conventional serpentine flow field their performances were evaluated under the same operating

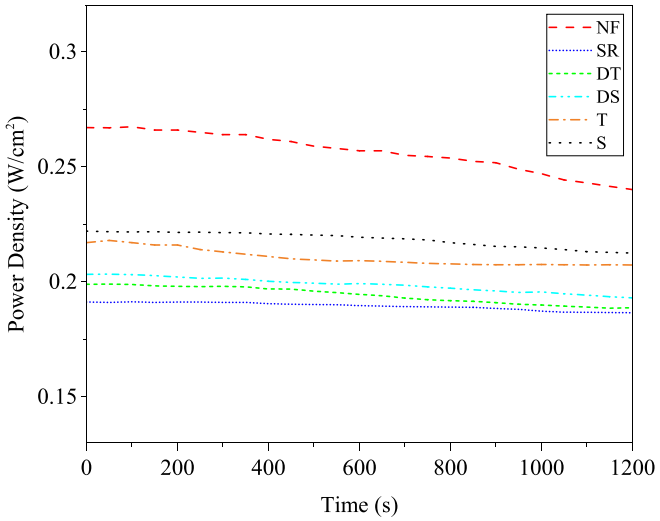


Fig. 9. Power density variation when operating at constant voltage.

parameters. The main findings are listed below:

- Performance tests were performed for single cell and the highest power density was achieved with NF-serpentine FF with 0.267 W/cm^2. Afterward, the S (0.225 W/cm^2) and T (0.219 W/cm^2) designs gave the highest power outputs. The single-cell performance tests yielded that any addiction or disturbance to the serpentine flow field affected positively and increased the net power output.
- The S and T obstacles created within the serpentine flow channel, which affect the performance increase, cause the rapid movement of the reactant gases to partially remove the water droplets quickly. In addition, the location of the DS and DT obstacles allows the water to remove the droplets from growth in the parts close to the GDL surface. Rapid transport was achieved thanks to the increased contact areas of the droplet size, air flow rate, and GDL surface. Interestingly, the NF placed within the serpentine channel dimensions was higher than the performance gain of the blocked flow areas inside the channel. The maximum effect of this situation can be attributed to the homogeneous distribution of the reactants and the removal of water without allowing the droplets to grow.
- EIS was performed to investigate the resistance losses of the cell during the test, and the measured values are at very low levels. Nevertheless, the lowest was measured with NF-serpentine FF due to the prevention of gas flow in the channel and providing homogeneous distribution throughout the active area.
- The expected result of the serpentine flow channel and its derivatives is a high level of pressure loss. Pressure losses in the designed FFs were determined and compared. Traditional coil FF, by its nature, provides the lowest pressure drop of 0.55 kPa. Obstacles in the flow channel were blocking the flow path and resisting the flow. Accordingly, they increased the pressure difference between the entry and exit points of the gases. The highest pressure drop was measured as 4.255 kPa in the NF-coil FF pair. Another feature of the current study is the relationship between performance change and pressure difference results. In general, the increase in pressure difference also increased the net power density. Accordingly, pressure drop measurements vary in proportion to the increase in performance.
- After the study, the least power density change of 2.6 % was observed in the serpentine flow field design, while the highest power density change of 10 % was observed in the NF structure placed in the serpentine channel. The change is relatively valid for short-term cell studies of 1200 s.

Net power densities are increased by creating a bipolar flow channel from a copper plate, which is not widely used, and NF positioning with a simple method. The most important feature here is to remove the contact resistance of water droplets formed on the GDL surface by increasing the reactant speeds. For this purpose, initially optimum flow rates and constant increasing speed values were provided. In order to obtain more accurate results, tests will be carried out by creating flow obstacles in different shapes and locations, taking these into account in the next study. Additionally, the width and length of flow barriers will be changed and investigated comprehensively. Thus, more comprehensive models of water management in serpentine-type flow fields commonly used for PEMFC operation need to be presented through experimental study.

CRediT authorship contribution statement

Selahattin Çelik: . **Mikail Yagiz:** Methodology. **Fuat Yildirim:** Formal analysis. **Alparslan Topcu:** Writing – original draft.

Declaration of Competing Interest

The authors declare that they have no known competing financial interests or personal relationships that could have appeared to influence the work reported in this paper.

Data availability

No data was used for the research described in the article.

References

[1] Chadha K, Martemianov S, Thomas A. Study of new flow field geometries to enhance water redistribution and pressure head losses reduction within PEM fuel cell. Int J Hydrogen Energy 2021;46(10):7489–501.
[2] Atyabi SA, Afshari E. Three-dimensional multiphase model of proton exchange membrane fuel cell with honeycomb flow field at the cathode side. J Clean Prod 2019;214:738–48.
[3] Chen X, Yu Z, Yang C, Chen Y, Jin C, Ding Y, et al. Performance investigation on a novel 3D wave flow channel design for PEMFC. Int J Hydrogen Energy 2021;46(19):11127–39.
[4] Guo Q, Qin Y. Numerical investigation of water droplet removal characteristics in novel block channels of PEMFC using dynamic wettability model. Int J Hydrogen Energy 2021;46(74):36890–902.
[5] Anyanwu IS, Xie X, Liu Z, Jiao K. Experimental investigation and optimization of proton exchange membrane fuel cell using different flow fields. Energy 2021;217:119313.
[6] Zhou Y, Chen B, Chen W, Deng Q, Shen J, Tu Z. A novel opposite sinusoidal wave flow channel for performance enhancement of proton exchange membrane fuel cell. Energy 2022;261:125383.
[7] Zhou Y, Chen B, Meng K, Zhou H, Chen W, Zhang N, et al. Optimal design of a cathode flow field for performance enhancement of PEM fuel cell. Appl Energy 2023;343:121226.
[8] Zhou Y, Meng K, Chen W, Deng Q, Chen B. Experimental performance of proton exchange membrane fuel cell with novel flow fields and numerical investigation of water-gas transport enhancement. Energ Conver Manage 2023;281:116865.
[9] Weng F-B, Dlamini MM, Hwang J-J. Evaluation of flow field design effects on proton exchange membrane fuel cell performance. Int J Hydrogen Energy 2023;48(39):14866–84.
[10] Wan Z, Yan H, Sun Y, Yang C, Chen X, Kong X, et al. Thermal management improvement of air-cooled proton exchange membrane fuel cell by using metal foam flow field. Appl Energy 2023;333:120642.
[11] Qin Z, Huo W, Bao Z, Tongsh C, Wang B, Du Q, et al. Alternating flow field design improves the performance of proton exchange membrane fuel cells. Adv Sci 2023;10(4):2205305.
[12] Valiño L, Mustata R, Gil MI, Martín J. Effect of the relative position of oxygen–hydrogen plate channels and inlets on a PEMFC. Int J Hydrogen Energy 2010;35(20):11425–36.
[13] Chowdhury MZ, Akansu YE. Novel convergent-divergent serpentine flow fields effect on PEM fuel cell performance. Int J Hydrogen Energy 2017;42(40):25686–94.
[14] Lin P, Wang H, Wang G, Li J, Sun J. Numerical study of optimized three-dimension novel Key-shaped flow field design for proton exchange membrane fuel cell. Int J Hydrogen Energy 2022;47(8):5541–52.
[15] Dong P, Xie G, Ni M. The mass transfer characteristics and energy improvement with various partially blocked flow channels in a PEM fuel cell. Energy 2020;206:117977.
[16] Hsieh S-S, Her B-S, Huang Y-J. Effect of pressure drop in different flow fields on water accumulation and current distribution for a micro PEM fuel cell. Energ Conver Manage 2011;52(2):975–82.
[17] Kerkoub Y, Benzaoui A, Haddad F, Ziari YK. Channel to rib width ratio influence with various flow field designs on performance of PEM fuel cell. Energ Conver Manage 2018;174:260–75.
[18] He L, Hou M, Gao Y, Sun X, Song W, Zheng L, et al. Experimental study of the S-shaped flow fields in proton exchange membrane fuel cells. Energ Conver Manage 2020;223:113292.
[19] Dong P, Xie G, Ni M. Improved energy performance of a PEM fuel cell by introducing discontinuous S-shaped and crescent ribs into flowing channels. Energy 2021;222:119920.
[20] Wang X, Qin Y, Wu S, Shangguan X, Zhang J, Yin Y. Numerical and experimental investigation of baffle plate arrangement on proton exchange membrane fuel cell performance. J Power Sources 2020;457:228034.
[21] Chen H, Guo H, Ye F, Ma CF. An experimental study of cell performance and pressure drop of proton exchange membrane fuel cells with baffled flow channels. J Power Sources 2020;472:228456.
[22] Shen J, Zhengkai Tu, Chan SH. Enhancement of mass transfer in a proton exchange membrane fuel cell with blockage in the flow channel. Appl Therm Eng 2019;149:1408–18.
[23] Wilberforce T, El Hassan Z, Ogungbemi E, Ijaodola O, Khatib FN, Durrant A, et al. A comprehensive study of the effect of bipolar plate (BP) geometry design on the performance of proton exchange membrane (PEM) fuel cells. Renew Sustain Energy Rev 2019;111:236–60.
[24] Wang Z, Tongsh C, Wang B, Liu Z, Du Q, Jiao K. Operation characteristics of open-cathode proton exchange membrane fuel cell with different cathode flow fields. Sust Energy Technol Assess 2022;49:101681.

[25] Ramin F, Sadeghifar H, Torkavannejad A. Flow field plates with trap-shape channels to enhance power density of polymer electrolyte membrane fuel cells. Int J Heat Mass Transf 2019;129:1151–60.
[26] He L, Hou M, Gao Y, Fang D, Wang P, Lv B, et al. A novel three-dimensional flow field design and experimental research for proton exchange membrane fuel cells. Energ Conver Manage 2020;205:112335.
[27] Palaniswamy K, Marappan M, Jothi VR. Influence of porous carbon inserts on scaling up studies for performance enhancement on PEMFC. Int J Hydrogen Energy 2016;41(4):2867–74.
[28] Hydrogen Air Mea–5Layer. <https://www.fuelcellstore.com/fuel-cell-components/membrane-electrode-assembly/hydrogen-air-mea>. [Accessed on 23.05.2023].
[29] Topcu A, Aydın K, Çelik S. The effect of the heater and the pump operation durations on the cold start performance of the coolant heating assisted PEM fuel cell application. Int J Energy Res 2022;46(15):23939–62.
[30] Coppo M, Siegel NP, Von Spakovsky MR. On the influence of temperature on PEM fuel cell operation. J Power Sources 2006;159(1):560–9.
[31] Abdulla S, Patnaikuni VS. Enhanced cross-flow split serpentine flow field design for square cross-sectional polymer electrolyte membrane fuel cell. Electrochim Acta 2021;391:138884.
[32] Pérez-Page M, Pérez-Herranz V. Effect of the operation and humidification temperatures on the performance of a pem fuel cell stack on dead-end mode. Int J Electrochem Sci 2011;6(2):492–505.
[33] Zhang G, et al. Optimization design of a parallel flow field for PEMFC with bosses in flow channels. Energies 2023;16(14):5492.
[34] Hsieh S-S, et al. Study of operational parameters on the performance of micro PEMFCs with different flow fields. Energ Conver Manage 2006;47(13-14):1868–78.
[35] Liu X, Guo H, Ma C. Water flooding and two-phase flow in cathode channels of proton exchange membrane fuel cells. J Power Sources 2006;156(2):267–80.
[36] Badduri SR, Naga Srinivasulu G, Srinivasa Rao S. Experimental analysis of PEM fuel cell performance using lung channel design bipolar plate. Int J Green Energy 2019;16(15):1591–601.
[37] Siefert NS, Litster S. Voltage loss and fluctuation in proton exchange membrane fuel cells: the role of cathode channel plurality and air stoichiometric ratio. J Power Sources 2011;196(4):1948–54.
[38] Heidary H, Kermani MJ, Advani SG, Prasad AK. Experimental investigation of in-line and staggered blockages in parallel flowfield channels of PEM fuel cells. Int J Hydrogen Energy 2016;41(16):6885–93.
[39] Ghanbarian A, Jafar Kermani M. Enhancement of PEM fuel cell performance by flow channel indentation. Energ Conver Manage 2016;110:356–66.
[40] Guo Q, Qin Y. Numerical investigation of water droplet removal characteristics in novel block channels of PEMFC using dynamic wettability model. Int J Hydrogen Energy 2021;46(74):36890–902.
[41] Bao Y, Gan Y. Roughness effects of gas diffusion layers on droplet dynamics in PEMFC flow channels. Int J Hydrogen Energy 2020;45(35):17869–81.
[42] Wang Y, Guan C, Zhang P, Zhu T, Wang S, Zhu Y, et al. Optimal design of a cathode flow field with a new arrangement of baffle plates for a high clean power generation of a polymer electrolyte membrane fuel cell. J Clean Prod 2022;375:134187.
[43] Chen H, Guo H, Ye F, Ma CF. 'An experimental study of cell performance and pressure drop of proton exchange membrane fuel cells with baffled flow channels'. J Power Sources 2020;472:228456.
[44] Iranzo A, Boillat P, Biesdorf J, Tapia E, Salva A, Guerra J. 'Liquid water preferential accumulation in channels of PEM fuel cells with multiple serpentine flow fields'. Int J Hydrogen Energy 2014;39(28):15687–95.
[45] Xie X, Zhou J, Wu S, Park JW, Jiao K. 'Experimental investigation on the performance and durability of hydrogen AEMFC with electrochemical impedance spectroscopy'. Int J Energy Res 2019;43(14):8522–35.